

Electron-Bernstein-Wave Current Drive in an Overdense Plasma at the Wendelstein 7-AS Stellarator

H. P. Laqua, H. Maassberg, N. B. Marushchenko, F. Volpe, A. Weller, and W7-AS Team
Max-Planck-Institut für Plasmaphysik, EURATOM Association, D-17491 Greifswald, Germany

W. Kasperek and ECRH-Group

Institut für Plasmaforschung, Universität Stuttgart, D-70569 Stuttgart, Germany

(Received 3 September 2002; published 21 February 2003)

Electron-Bernstein-wave (EBW) current drive in an overdense plasma was demonstrated at the Wendelstein 7-AS stellarator for the first time. The EBWs were generated by O-X-B mode conversion. The relatively high current drive efficiency was consistent with theoretical predictions. The experiments provided first investigations of EBW phase space interaction for wave refractive indices much larger than unity.

DOI: 10.1103/PhysRevLett.90.075003

PACS numbers: 52.55.Hc, 52.35.Hr, 52.50.Sw, 52.55.Wq

Introduction.—The experiments reported here represent both the first measurement of electron-Bernstein-wave current drive (EBCD) in an overdense fusion plasma and the first experimental test of the theory of electron-Bernstein-wave (EBW) phase space interaction. Efficient noninductive current drive (CD) may allow steady state operation of tokamaks as a fusion reactor. In addition, localized off-axis current drive can be used for q -profile shaping and neoclassical tearing mode stabilization [1]. Moreover, for high-density operation and in spherical tokamaks such as NSTX the plasma density can exceed the accessible plasma density for electron cyclotron current drive (ECCD) with electromagnetic waves. For the electrostatic EBW no upper limit exists. Even more, due to their electrostatic character EBW's can achieve parallel refractive indices (N_{\parallel}) larger than 1. This makes the EBW's an attractive candidate for efficient current drive as postulated by Litvak *et al.* [2].

However, since EBW's cannot propagate in the vacuum, they have to be converted from electromagnetic waves first. This can be performed by the O-X-B mode conversion process, which was proposed by Preinhaelter *et al.* [3] and demonstrated for fusion plasma heating by Laqua [4]. The EBW's propagate then towards the dense plasma center where they are absorbed by cyclotron damping. The mode conversion process requires an optimal parallel component $N_{\parallel, \text{optimal}}$ of the vacuum refractive index vector, or, equivalently, an oblique optimal launch angle φ , a plasma density above the O-wave cutoff and a frequency above the first cyclotron harmonic in the plasma. However, the refractive index of Bernstein waves strongly depends on the magnetic field and can be changed by the magnetic field shear, curvature, and gradient [5,6]. This makes the efficiency and profile of CD very sensitive to the configuration.

Stellarators are ideal devices for CD measurement, even though they have little necessity for CD. However, due to the possibility of currentless operation, even small

external current can be measured precisely. Stellarators also do not suffer from a density limit based upon stability, which makes them an ideal tool for investigation of wave physics in overdense plasmas. Furthermore, the three-dimensional magnetic configuration gives an experimental flexibility, which is not attainable in tokamaks. Finally, both the wave propagation and the wave particle interaction are based on the local plasma parameters; therefore the results are transferable to tokamaks.

Experimental setup.—Two kinds of experiments were performed at the Wendelstein 7-AS stellarator [7]: (1) In “current-free” discharges the plasma current was compensated for by an inductive current of a feedback controlled transformer. (2) The plasma current was able to freely develop.

The microwave beam was launched from a 70 GHz gyrotron with up to 450 kW power via an optical transmission line and a movable launch mirror into a target plasma at a density n_e of around $1.05 \times 10^{20} \text{ m}^{-3}$. The target was sustained by neutral beam injection (NBI) with up to 0.8 MW power which provides a flat density profile in the core and a local density scale length of 1 cm at the O-X conversion layer at the edge. Since the current drive efficiency scales as T_e/n_e the density was set to the lowest value where efficient O-X-B conversion can be achieved, which is about 1.5 the plasma cutoff density. Here the O-X-B conversion was experimentally optimized with respect to the angular window necessary for efficient EBW generation by scanning both the toroidal and poloidal launch angle. Further the pure O-mode polarization was checked. The optimization criterion was the increase of plasma energy and the reduction of the nonabsorbed stray radiation [8]. The magnetic field was adjusted to 2.15 T on axis at the toroidal launch position to get central power deposition. Here the large N_{\parallel} component of the EBW's requires a stronger reduction of the resonant magnetic field than for standard ECCD. In current-free discharges all the contributions

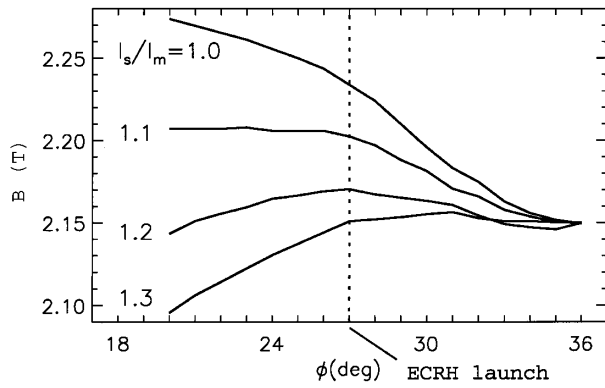


FIG. 1. Variation of the on-axis magnetic field versus the toroidal angle for different ratios of coil currents. The ECRH antenna was located at 27° toroidal angle.

to the plasma current, namely, the bootstrap current (BSC), the current driven by NBI (NBCD), and the EBW driven current (EBCD) were compensated by the inductive current. The loop voltage U_{loop} is then a measure for the plasma currents:

$$U_{loop} = -R_{plasma}(I_{BSC} + I_{NBCD} \pm I_{EBCD}).$$

R_{plasma} represents the plasma resistance and the positive and negative signs before I_{EBCD} correspond to co- and counter-EBCD, respectively. Since the launch angle was fixed by the O-X-B-mode conversion condition, a variation of $N_{||}$ at the EC-absorption zone was possible only by changing the magnetic configuration.

In contrast to a tokamak, in a stellarator the magnetic field on axis varies with the toroidal position, as shown in Fig. 1. By changing the ratio of different coil currents (“mirror ratio” I_s/I_m), a minimum or maximum of the magnetic field can be created near the HF power launch position. In Fig. 2 ray-tracing calculations of EBW propa-

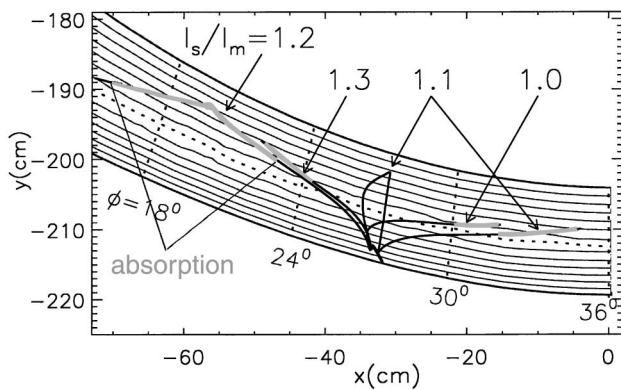


FIG. 2. Ray trajectories (black lines) in the equatorial plane for different mirror ratios I_s/I_m . Φ is the toroidal angle; x and y are the spatial coordinates. The dashed line represents the plasma center; the grey lines are the cuts through the flux surfaces. The thick grey parts of the ray traces indicate the region where 99% of the power is lost by cyclotron absorption.

gation for different mirror ratios are shown. Figure 3 illustrates the associated variation of $N_{||}$. For a local minimum ($I_s/I_m \leq 1.0$) starting at the initial value of -0.6 (O-X-B process) $N_{||}$ crosses 0 and attains $N_{||} > 1$. Here the EBW’s are absorbed by cyclotron interaction. For a local maximum of B ($I_s/I_m \geq 1.2$) the $N_{||}$ remains negative but reaches $N_{||} < -1$. A detailed description of the hot plasma 3D ray-tracing code is given in [9,10]. In Fig. 4 loop voltage signals for discharges with mirror ratios of 1.0 and 1.2 are shown. According to the sign of the final $N_{||}$ the loop voltage change is positive for co-EBCD or negative for counter-EBCD. The reason for the positive sign of U_{loop} is that these experiments had been performed at a negative magnetic field in our sign convention. The estimation of the total EBW current in the background of I_{BSC} and I_{NBCD} is rather uncertain since the change of U_{loop} due to EBCD is of the same order as the error bars for the calculated U_{loop} of all other current contributions. Even in the absence of EBCD the temperature increase due to EBW heating changes I_{BSC} , I_{NBCD} , and R_{plasma} . For that reason the analysis was not based on the total U_{loop} value, but on its variation at the EBCD switch-on and switch-off. Therefore the calculated U_{loop} associated with the other currents was adjusted within its error bars to the U_{loop} measured before EBCD switch-on. Further, in the high-density discharge the plasma parameters could not be held completely stationary. Nevertheless, to get a sufficiently precise estimation of the different contribution to the loop voltage, the plasma currents were calculated for a large parameter range in the electron temperature T_e , density n_e , and the effective charge Z_{eff} . The functional dependencies on these parameters were found by a three-dimensional least squares fit. With this, the time slope of the loop voltage could be calculated as a function of the plasma parameters. The T_e and n_e profiles were measured with the Thomson scattering every 50 ms. For the time in between, the temporal evolution of T_e and n_e was inferred using the SoftX-filter methods and the microwave interferometer, respectively. Additionally, to improve the calibration of the Thomson

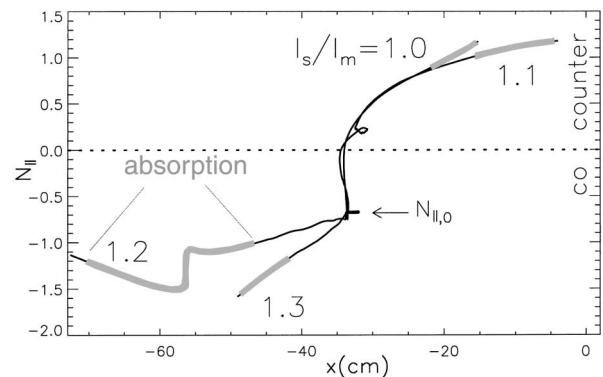


FIG. 3. Evolution of $N_{||}$ for different ray trajectories according to Fig. 2.

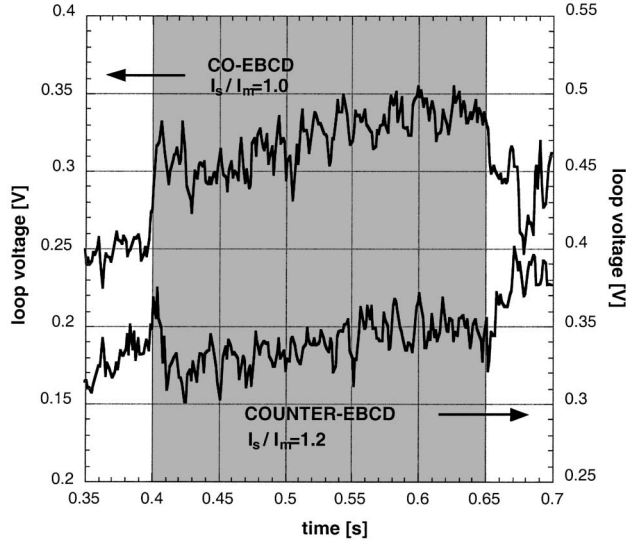


FIG. 4. Change of loop voltage during co- and counter-EBCD (0.4–0.65 s). Since the magnetic configuration was different for the two cases, the signals refer to different scales.

scattering the n_e profile was calibrated according to the cutoff for the second harmonic extraordinary mode (X mode), as detected by the electron cyclotron emission radiometer. The Z_{eff} slope was calculated from the bremsstrahlung intensity. Its value varied around 1.5. As shown in Fig. 4 the experimental time slope of the loop voltage could be reproduced by the calculations. Here also the response of the feedback control system was taken into account to reproduce the fast changes of the loop voltage. Finally, a dimensionless EBCD efficiency [11] of

$$\zeta = \frac{e^2 I_{\text{CD}} n_e R_0}{\epsilon_0^2 P_{\text{HF}} T_e} = 0.43 \pm 0.1 \left(\frac{I_{\text{CD}}}{P_{\text{HF}}} \left[\frac{\text{kA}}{\text{kW}} \right], \frac{n_e R_0}{T_e} \left[\frac{10^{20}}{\text{m}^2 \text{eV}} \right] \right)$$

could be estimated for both the co- and counter-EBCD cases. Here I_{CD} , P_{HF} , and R_{oh} represent driven current, the electrical charge, the dielectric constant, the HF power, and the major plasma radius. In numbers this efficiency gives a current of 2 ± 0.5 kA for 400 kW HF power at a density of $1.05 \times 10^{20} \text{ m}^{-3}$ and a temperature of 800 eV. Without EBCD the change of plasma temperature would lead to an increase of U_{loop} which is in contradiction with the measurement as shown in Fig. 5. The dimensionless CD efficiency was chosen because it takes into account the effects of trapped particles, which are also relevant for off-axis ECCD in tokamaks [11] (trapped particles are those which are confined in a local magnetic minimum due to the conservation of energy and magnetic momentum). A comparison with other CD methods such as lower hybrid waves or ion cyclotron waves, for example, is relevant only if the results of the low temperature experiments ($T_e = 0.8$ keV) are extrapolated to typical fusion

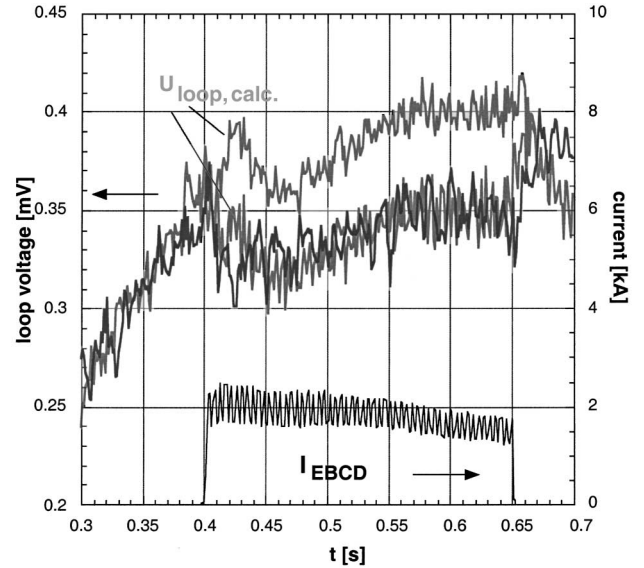


FIG. 5. Calculated loop voltages (grey) for EBW heating only (top trace) and with additional countercurrent drive (lower trace) in comparison with the measured loop voltage (black curve). The consistency with the measured loop voltage yields a dimensionless CD efficiency $\zeta = 0.43$. The resulting EBCD current (bottom trace) is then a function of T_e , n_e , and P_{HF} . The latter was modulated with 20% amplitude.

plasma parameters ($T_e = 8$ keV). Then the usually used CD efficiency $\gamma = n_e R I_{\text{CD}} / P_{\text{HF}} = 0.1$ would become compatible with the other CD methods.

In the second type of experiments the plasma parameters were set such that bootstrap current was approximately compensated by counter-NBCD. Here the current feedback control was switched off and the plasma current rose up to 1.2 kA during EBW heating on the L/R_{plasma} time scale of the plasma as shown in Fig. 6. Because of the limited pulse length the stationary condition could not be reached. The plasma parameters were $n_e = 1.2 \times 10^{20} \text{ m}^{-3}$ and $T_e = 500$ eV. This result confirms the CD efficiency of the current-free-type experiments.

Numerical simulation.—For the experimental plasma parameters and for the calculated N vector Fokker-Planck calculations were performed to estimate the distortion of the electron distribution function. Because of a large N_{\parallel} value and to the associated strong Doppler shift, the EC interaction took place at more than 2 times the thermal velocity. Thus the quasilinear diffusion is situated far away from the trapped electron loss cone, as illustrated in Fig. 7. Further, the resonance curve is no longer an ellipse as for $|N_{\parallel}| < 1$ but becomes a parabola for $|N_{\parallel}| = 1$ and a hyperbola for $|N_{\parallel}| > 1$. The perpendicular refractive index N_{\perp} is about 40, which means that the wavelength is of the order of the gyroradius or even smaller. In that case the quasilinear diffusion operator splits into many maxima and the interaction takes place

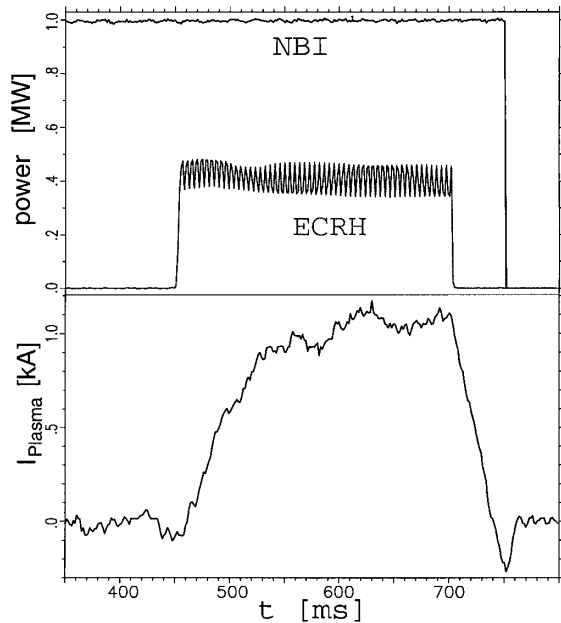


FIG. 6. Top: power signals for NBI and ECRH. Bottom: plasma current during EBCD.

even with the high energy suprathermal electrons (see Fig. 7). For the experimental parameters driven currents of 2.3 kA for co-EBCD and 3.7 kA for counter-EBCD were predicted, which overestimate the experimental results by a factor of up to 1.8. Since these calculations are based on the assumption of one ideal single ray, ignoring the broader power deposition of a real beam, this result must be considered as a theoretical limit. Nevertheless the favorable properties of the EBWs for current drive are evident from Fokker-Planck calculation.

In this calculation also a suprathermal population for electrons with 5 times the thermal energy is predicted. Experimental hints for this suprathermal population could be found in T_e measurements from the SoftX emission with the filter method. Three central lines of sight were equipped with pairs of Be filters of different thickness. Therefore the temperature was determined at different electron energies. Before the EBCD the SoftX temperatures were approximately equal at 740 eV. As EBCD was switched on the x-ray filter method yielded a rise of T_e , which increases with the thickness of the filter pairs corresponding to the shift of the spectral range to higher electron energies. In numbers, the temperature increases by 55, 95, and 145 eV for an electron energy of 2.7, 3.9, and 5.7 times T_e . This is attributed to a non-Maxwellian tail which is unaccounted for in the T_e analysis.

Conclusions.—Noninductive current drive with electron Bernstein waves in an overdense plasma was experi-

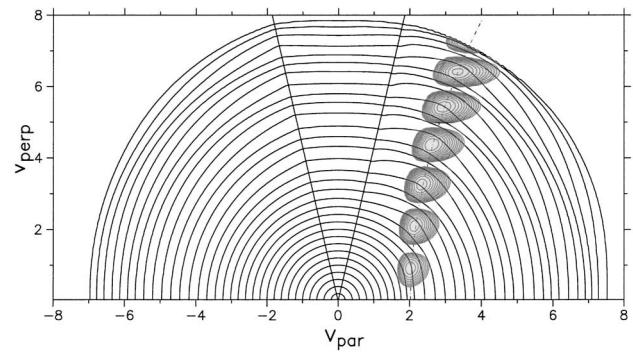


FIG. 7. Contours of the electron distribution function in a logarithmic scale as a function of the parallel velocity V_{par} and of the perpendicular velocity V_{perp} . Both are normalized to the thermal velocity. The grey structure is the quasilinear diffusion operator for EBWs with $N_{\parallel} = 1.0$. The calculation was limited to $|V| < 8V_{\text{thermal}}$.

mentally demonstrated at Wendelstein7-AS for the first time. The EBWs were generated by O-X-B mode conversion. Their N_{\parallel} value could be varied from below -1 to above 1 by varying the magnetic configuration. For both the co- and counterdirection about 2 kA of driven current was found. The dimensionless CD efficiency exceeds those of standard ECCD by a factor of 2–3. This was confirmed by Fokker-Planck calculations, which show also the new features of the phase space interaction for large wave refractive indices. In comparison with standard ECCD, for EBCD the phase space interaction is far away from the trapped electrons and mainly suprathermal electrons are involved.

-
- [1] G. Gantenbein *et al.*, Phys. Rev. Lett. **85**, 1242 (2000).
 - [2] A. G. Litvak *et al.*, Phys. Lett. A **188**, 64 (1994).
 - [3] J. Preinhaelter and V. Kopecký, J. Plasma Phys. **10**, 1 (1973).
 - [4] H. P. Laqua *et al.*, Phys. Rev. Lett. **78**, 3467 (1997).
 - [5] C. B. Forest *et al.*, Phys. Plasmas **7**, 1352–1354 (2000).
 - [6] T. Meakawa *et al.*, Phys. Rev. Lett. **86**, 3783 (2001).
 - [7] H. Renner *et al.*, Plasma Phys. Controlled Fusion **31**, 1579 (1989).
 - [8] H. P. Laqua *et al.*, in *Proceedings of the 28th European Physical Society Conference on Controlled Fusion and Plasma Physics, Funchal (Madeira), 2001*, edited by C. Silva, C. Varandas, and D. Campbell (European Physical Society, Lisbon, 2001), p. 3.099.
 - [9] F. Volpe and H. P. Laqua, Rev. Sci. Instrum. (to be published).
 - [10] F. Volpe, Ph.D. thesis, Ernst Moritz Arndt University Greifswald, 2002.
 - [11] T. C. Luce *et al.*, Phys. Rev. Lett. **83**, 4550 (1999).